J|A|C|S
ARTICLES
Published on Web 02/20/2007

Forming Biocompatible and Nonaggregated Nanocrystals in Water Using Amphiphilic Polymers

William W. Yu,[†] Emmanuel Chang,[‡] Joshua C. Falkner,[†] Junyan Zhang,[†] Ali M. Al-Somali,[†] Christie M. Sayes,[†] Judah Johns,[†] Rebekah Drezek,[‡] and Vicki L. Colvin*,[†]

Contribution from the Departments of Chemistry and Bioengineering, Rice University, Houston, Texas 77005

Received October 6, 2006; E-mail: colvin@rice.edu

Abstract: High-quality nanocrystals formed in organic solvents can be completely solubilized in water using amphiphilic copolymers containing poly(ethylene glycol) or PEG. These copolymers are generated using a maleic anhydride coupling scheme that permits the coupling of a wide variety of PEG polymers, both unfunctionalized and functionalized, to hydrophobic tails. Thermogravimetric analysis, size exclusion chromatography, cryogenic transmission electron microscopy, and infrared spectroscopy all indicate that the copolymers effectively coat the nanocrystals surfaces. The composite nanocrystal−polymer assemblies can be targeted to recognize cancer cells with Her2 receptor and are biocompatible if their surface coatings contain PEG. In the particular case of semiconductor nanocrystals (e.g., quantum dots), the materials in water have the same optical spectra as well as quantum yield as those formed initially in organic solutions.

Introduction

The unique and tunable optical, magnetic, and chemical features of nanocrystals are finding increasing use in medicine, where they have been shown to improve the diagnosis, imaging, and treatment of disease.[1−9] In such applications, semiconductor and ceramic nanocrystals are typically fashioned as dispersed and nonaggregated particles that, by virtue of their small size, have wide distribution and effect in biological systems. General, cost effective, and versatile methods for forming such isolated nanoparticles and characterizing their hydrodynamic size, surface composition, and concentration remain a major challenge for the area. In this work, we present a versatile coating strategy that can effectively phase transfer into biological fluids the monodisperse nanocrystals best formed in organic solutions at high temperatures.[10−17] These inorganic−organic particles are evaluated using a suite of techniques which together provide a structure for these materials as well as a measure of their biological activity.

Engineering nanocrystal coatings for biological applications is a significant challenge since narrow distribution and highly crystalline nanocrystals are best formed in organic solutions and as a result are stabilized with hydrophobic functionalities.[10−17] Any strategy aimed at using these systems in biological applications must somehow transform these surface coatings into hydrophilic and ideally biocompatible species. In one approach, ligand exchange reactions strip the nanocrystal surface of their original hydrophobic coatings, replacing them with bifunctional capping molecules or an inorganic coating such as silica.[18−23] Because the optical and magnetic properties of the inorganic core are often very sensitive to the surface, this process can result in poorer performance, particularly in the case of quantum dots (QDs).[24]

A second approach is to encapsulate the nanocrystals in an amphiphile whose hydrophobic ends interleave with, but not

[†] Department of Chemistry.
[‡] Department of Bioengineering.

(1) Wu, X.; Liu, H.; Liu, J.; Haley, K. N.; Treadway, J. A.; Larson, J. P.; Ge, N.; Peale, F.; Bruchez, M. P. *Nat. Biotechnol.* **2003**, *21*, 41−46.
(2) Dahan, M.; Levi, S.; Luccardini, C.; Rostaing, P.; Riveau, B.; Triller, A. *Science* **2003**, *302*, 442−445.
(3) Lidke, D.; Nagy, P.; Heintzmann, R.; Arndt-Jovin, D.; Post, J.; Grecco, H.; Jares-Erijman, E.; Jovin, T. *Nat. Biotechnol.* **2004**, *22*, 198−203.
(4) Roth, J. *Histochem. Cell Biol.* **1996**, *106*, 1−8.
(5) Schulze, E.; Ferrucci, J.; Poss, K.; Lapointe, L.; Bogdanova, A.; Weissleder, R. I. R. *Invest. Radiol.* **1995**, *30*, 604−610.
(6) Alivisatos, P. *Nat. Biotechnol.* **2004**, *22*, 47−52.
(7) Alivisatos, A. P.; Gu, W.; Larabell, C. *Annu. Rev. Biomed. Eng.* **2005**, *7*, 55−76.
(8) Miyawaki, A.; Sawano, A.; Kogure, T. *Nat. Cell Biol.* **2003**, *5* (Suppl), S1−S7.
(9) Niemeyer, C. M. *Angew. Chem., Int. Ed.* **2001**, *40*, 4128−4158.
(10) Murray, C. B.; Norris, D. J.; Bawendi, M. G. *J. Am. Chem. Soc.* **1993**, *115*, 8706−8715.
(11) Peng, Z. A.; Peng, X. *J. Am. Chem. Soc.* **2001**, *123*, 183−184.
(12) Yu, W. W.; Wang, Y. A.; Peng, X. *Chem. Mater.* **2003**, *15*, 4300−4308.
(13) Yu, W. W.; Peng, X. *Angew. Chem., Int. Ed.* **2002**, *41*, 2368−2371.
(14) Battaglia, D.; Peng, X. *Nano Lett.* **2002**, *2*, 1027−1030.
(15) Yu, W. W.; Falkner, J. C.; Shih, B. S.; Colvin, V. L. *Chem. Mater.* **2004**, *16*, 3318−3322.
(16) Bailey, R. E.; Nie, S. *J. Am. Chem. Soc.* **2003**, *125*, 7100−7106.
(17) Kim, S.; Lim, Y. T.; Soltesz, E. G.; De Grand, A. M.; Lee, J.; Nakayama, A.; Parker, J. A.; Mihaljevic, T.; Laurence, R. G.; Dor, D. M.; Cohn, L. H.; Bawendi, M. G.; Frangioni, J. V. *Nat. Biotechnol.* **2004**, *22*, 93−97.
(18) Gerion, D.; Pinaud, F.; Williams, S. C.; Parak, W. J.; Zanchet, D.; Weiss, S.; Alivisatos, A. P. *J. Phys. Chem. B* **2001**, *105*, 8861−8871.
(19) Bruchez, M., Jr.; Moronne, M.; Gin, P.; Weiss, S.; Alivisatos, A. P. *Science* **1998**, *281*, 2013−2016.
(20) Selvan, S. T.; Tan, T. T.; Ying, J. Y. *Adv. Mater.* **2005**, *17*, 1620−1625.
(21) Gomez, D. E.; Pastoriza-Santos, I.; Mulvaney, P. *Small* **2005**, *1*, 238−241.
(22) Mulvaney, P.; Liz-Marzan, L. M.; Giersig, M.; Ung, T. *J. Mater. Chem.* **2000**, *10*, 1259−1270.
(23) Nann, T.; Mulvaney, P. *Angew. Chem., Int. Ed.* **2004**, *43*, 5393−5396.
(24) Rogach, A. L.; Nagesha, D.; Ostrander, J. W.; Giersig, M.; Kotov, N. A. *Chem. Mater.* **2000**, *12*, 2676−2685.

replace, the organic coating on a nanocrystal. Surfactants, such as phospholipids and α-cyclodextrin, are one example of such encapsulants, and they can successfully transfer nanocrystals into pure water. However, the materials are not generally stable in biological settings because of relatively weak anchoring of the single and double hydrophobic tails to the particle. Additionally, the hydrophilic end groups of even biocompatible surfactants may not protect nanocrystals from nonspecific biomolecular interactions.[25−30]

Many of these problems can be overcome by using amphiphilic polymers which in principle offer more potential for tailoring both the hydrophobic and hydrophilic interactions between particles and their coatings.[1,31,32] Because single polymer chains can contain multiple hydrophobic units, their interactions with the native organic coatings on nanocrystals can be numerous, and thus the encapsulant can be bound more strongly than conventional surfactants. In addition, the external functionality of the nanocrystal−polymer assembly can be widely varied through introduction of different amphiphilic moieties. Though promising for coating nanocrystals, amphiphilic polymers containing hydrophobic tails most conducive to particle stabilization are not available commercially. The few examples of their use to date have relied on coupling schemes that use reactive end groups (−SH, $-NH_2$) found only on a limited and expensive set of polymers. As a result, the range of amphiphilic polymers for creating stable and nonaggregating nanocrystals in biological settings has been relatively limited.

To fully explore the structure and optimize amphiphilic polymers for nanocrystal stabilization requires simple methods to generate amphiphilic polymers through coupling of single component hydrophobic and hydrophilic chains. Of particular interest for biocompatibility is the incorporation of poly(ethylene glycol) (PEG) into the surface coatings.[1,27,31,33] Nanocrystals that have PEG-functionalized exteriors exhibit generally much less toxicity and longer circulation time than water-soluble nanocrystals made with other agents.[26,27,34−37] The few schemes for producing such materials as part of amphiphilic polymers require the use of derivatized PEG polymers such as mPEG−NH_2 (primary amino group terminated poly(ethylene glycol) methyl ether) or PEG−SH.[1,27,31,33] These starting products are usually expensive and available in only a few molecular weights and with limited additional functionality for coupling (e.g., −COOH moieties).

Here, we report a general method to form stable nanocrystals in water using amphiphilic polymers generated through simple and low cost methods.[32] Our amphiphilic coating agents are formed using a maleic anhydride coupling scheme that works both with mPEG−NH_2 and underivatized mPEG−OH (poly(ethylene glycol) methyl ether) as starting materials. Because these materials are available with a wide variety of chain lengths, we can compare how PEG size influences physiological stability as well as biocompatibility.[34,38,39] The method is quite general, and we demonstrate the technique using our model system of quantum dots as well as nanoscale Fe_3O_4. We characterize the molar concentration and hydrodynamic size of our solutions using multiple tools and also show that the PEG coatings produce materials that are nontoxic in cell culture.

Experimental Section

Quantum Dots. Three colors (red, yellow, and green) of QDs with core/shell structures were synthesized according to published methods but with modifications to the shell growth temperatures (CdSe as the core).[40] For this work, we used 180 °C for CdS shell growth (red and yellow QDs) and 200 °C for ZnS shell growth (green QD). All the QDs were purified and stored in chloroform before further treatment. QD concentrations were determined using the extinction coefficients, and the error in these measurements was estimated by comparing the wide range of reported extinction coefficients in the literature.[41−43]

Iron Oxide Nanocrystals. The formation of monodisperse iron oxide nanocrystals with various sizes (6−40 nm) relied on the high-temperature decomposition of iron carboxylate salts in octadecene (ODE).[44] Though the materials generated have a composition different from that of the quantum dots, the similarity in solvents and methods suggests that the surface coatings after formation are comparable in the two different systems.

Amphiphilic Polymers. Poly(maleic anhydride-alt-1-octadecene) (PMAO, M_n = 30 000−50 000, Aldrich, St. Louis, MO) reacted with primary amino group terminated poly(ethylene glycol) methyl ethers (mPEG−NH2, MW 6000, 9900, and 19 300; Nektar, San Carlos, CA) in chloroform (Fisher, Pittsburgh, PA) overnight (room temperature) to form amphiphilic polymers (PMAO−PEG) (molar ratio of PMAO/PEG ranged from 1:5 to 1:30). Poly(ethylene glycol) methyl ethers (mPEG−OH, MW 550, 750, and 2000 from Aldrich) are much more economical than mPEG−NH_2. They were also used to react with PMAO to make PMAO−PEG amphiphilic polymers; this approach required acid catalysis (e.g., several drops of concentrated H_2SO_4) and refluxing in chloroform at ∼61 °C for 12 h. The solution was neutralized by 1 M NaOH and then centrifuged to remove the salt (Na_2SO_4) and water.

Water-Soluble Nanocrystals. The monodisperse QDs (purified and dispersed in chloroform) and the amphiphilic polymer (PMAO−PEG)

(25) Aldana, J.; Wang, Y. A.; Peng, X. *J. Am. Chem. Soc.* **2001**, *123*, 8844−8850.
(26) Smith, A. M.; Duan, H.; Rhyner, M. N.; Ruan, G.; Nie, S. *Phys. Chem. Chem. Phys.* **2006**, *8*, 3895−3903.
(27) Bentzen, E. L.; Tomlinson, I. D.; Mason, J.; Gresch, P.; Warnement, M. R.; Wright, D.; Sanders-Bush, E.; Blakely, R.; Rosenthal, S. J. *Bioconjugate Chem.* **2005**, *16*, 1488−1494.
(28) Dubertret, B.; Skourides, P.; Norris, D. J.; Noireaux, V.; Brivanlou, A. H.; Libchaber, A. *Science* **2002**, *298*, 1759−1762.
(29) Fan, H.; Leve, E. W.; Scullin, C.; Gabaldon, J.; Tallant, D.; Bunge, S.; Boyle, T.; Wilson, M. C.; Brinker, C. J. *Nano Lett.* **2005**, *5*, 645−648.
(30) Wang, Y.; Wong, J. F.; Teng, X.; Lin, X. Z.; Yang, H. *Nano Lett.* **2003**, *3*, 1555−1559.
(31) Gao, X.; Cui, Y.; Levenson, R. M.; Chung, L. W. K.; Nie, S. *Nat. Biotechnol.* **2004**, *22*, 969−976.
(32) Pellegrino, T.; Manna, L.; Kudera, S.; Liedl, T.; Koktysh, D.; Rogach, A. L.; Keller, S.; Raedler, J.; Natile, G.; Parak, W. J. *Nano Lett.* **2004**, *4*, 703−707.
(33) Ballou, B.; Lagerholm, B. C.; Ernst, L. A.; Bruchez, M. P.; Waggoner, A. S. *Bioconjugate Chem.* **2004**, *15*, 79−86.
(34) Chang, E.; Thekkek, N.; Yu, W. W.; Colvin, V. L.; Drezek, R. *Small* **2006**, *2*, 1412−1417.
(35) Hoshino, A.; Fujioka, K.; Oku, T.; Suga, M.; Sasaki, Y. F.; Ohta, T.; Yasuhara, M.; Suzuki, K.; Yamamoto, K. *Nano Lett.* **2004**, *4*, 2163−2169.
(36) Derfus, A. M.; Chan, W. C. W.; Bhatia, S. N. *Nano Lett.* **2004**, *4*, 11−18.
(37) Kirchner, C.; Liedl, T.; Kudera, S.; Pellegrino, T.; Javier, A. M.; Gaub, H. E.; Stoelzle, S.; Fertig, N.; Parak, W. J. *Nano Lett.* **2005**, *5*, 331−338.
(38) Chang, E.; Miller, J. S.; Sun, J.; Yu, W. W.; Colvin, V. L.; Drezek, R.; West, J. L. *Biochem. Biophys. Res. Commun.* **2005**, *334*, 1317−1321.
(39) Chang, E.; Yu, W. W.; Colvin, V. L.; Drezek, R. *J. Biomed. Nanotechnol.* **2005**, *1*, 397−401.
(40) Li, J. J.; Wang, Y. A.; Guo, W.; Keay, J. C.; Mishima, T. D.; Johnson, M. B.; Peng, X. *J. Am. Chem. Soc.* **2003**, *125*, 12567−12575.
(41) Yu, W. W.; Qu, L.; Guo, W.; Peng, X. *Chem. Mater.* **2003**, *15*, 2854−2860 (Correction: *Chem. Mater.* **2004**, *16*, 560).
(42) Leatherdale, C. A.; Woo, W.-K.; Mikulec, F. V.; Bawendi, M. G. *J. Phys. Chem. B* **2002**, *106*, 7619−7622.
(43) Striolo, A.; Ward, J.; Prausnitz, J. M.; Parak, W. J.; Zanchet, D.; Gerion, D.; Milliron, D.; Alivisatos, A. P. *J. Phys. Chem. B* **2002**, *106*, 5500−5505.
(44) Yu, W. W.; Falkner, J. C.; Yavuz, C. T.; Colvin, V. L. *Chem. Commun.* **2004**, 2306−2307.

were mixed in chloroform and stirred overnight (room temperature) (molar ratio of QD/PMAO−PEG ranged from 1:5 to 1:30). After that, pure water was added to the chloroform solution of the complexes with at least a 1/1 volume ratio; chloroform was then gradually removed by rotary evaporation at room temperature and resulted in clear and colored solution of water-soluble QDs. This transfer process had a 100% efficiency, and no residue was observed; however, to remove possible larger contaminants the solutions were passed through a 0.2-μm Nylon syringe filter. An ultracentrifuge (Beckman Coulter Optima L-80XP) was used to further concentrate and purify (remove excess amphiphilic polymer) the materials (typically at 200000−300000*g* for 1 to 2 h). Water-soluble iron oxide nanocrystals were prepared and purified following the same procedure as described above for QDs.

Characterization of Nanocrystals. Ultraviolet−visible absorption spectra of QDs were measured by a Varian Cary 5000 UV−VIS−NIR spectrophotometer. Photoluminescence (PL) spectra of QDs were recorded on a Jobin Yvon Spex Fluorolog 3 fluorescence spectrophotometer. Infrared spectra (FTIR) were collected from films of dried solution on KBr crystals using Nicolet 760 spectrometer.

Regular TEM specimens were made by evaporating one drop of nanocrystal solutions on carbon-coated copper grids. The TEM micrographs were taken by Jeol FasTEM 2010 transmission electron microscope operating at 100 kV. The size and size distribution data were obtained by counting >1000 individual nanocrystalline particles using Image-Pro Plus 5.0 (Media Cybernetics, Inc., Silver Spring, MD).[15,44] Cryogenic-TEM (cryo-TEM) was used to observe the aggregation state of QDs and iron oxide nanocrystals in water solutions; the specimen was made by quickly freezing (by means of liquid nitrogen) a thin water film on a copper grid using a Vitrobot (FP5350/60; FEI, Hillsboro, OR) instrument. As has been widely established in biology, cryo-TEM completed under these conditions provides an accurate and complete picture of the solution-state structure of materials.[45,46]

Size exclusion chromatography (SEC) was applied to measure the hydrodynamic diameters of the water-soluble QDs on an Agilent high-performance liquid chromatograph (1100 series) equipped with hydroxylated polymethacrylate-based gel (Waters Corporation, Milford, MA; Ultrahydrogel 1000 and 2000) columns.[47,48] The mobile phase was a mixture of 15% acetonitrile and 85% water (containing 0.001 M sodium citrate dihydrate to suppress electrostatic interaction). The standard molecular weight curve was obtained using PEG standards (Polymer Laboratories, Amherst, MA; MW ranged from 106 to 1 215 000). Dynamic light scattering (DLS) was also employed to measure the hydrodynamic diameters of the water-soluble QDs, though it generally provided less quantitative data than that found using SEC. The results were obtained from Brookhaven 90plus particle analyzer at 25 °C.

Quantum Dot−Antibody Bioconjugates. The water-soluble QDs have many carboxylic groups on the polymer backbone that were generated during the reactions of maleic anhydride and the functional groups of the starting PEG polymers. Those free carboxylic groups react with biomolecules with amino groups to make QD bioconjugates.[1,31] One example shown here was to make QD−anti-Her2 antibody (LabVision, Fremont, CA) bioconjugates via EDC coupling at room temperature in 1X PBS buffer (pH = 6.8) for 2 h (molar ratio of QD/anti-Her2/EDC was 1:5:20). The water-soluble QDs used here were made using PMAO−PEGs with fewer PEG molecules (molar ratio of PMAO/PEG was 1:10) to avoid blocking the carboxylic groups. The QD−anti-Her2 bioconjugate products were left there for overnight (to quench the activated −COOH groups) and then used as is or purified by ultracentrifugation at 200000−300000*g* for 1 to 2 h. To avoid possible extended network aggregates via cross-coupling antibodies and QDs, we worked at a lower concentration of 0.1 μM QDs. A structure of QD−Au nanocrystals has been prepared to image proteolytic activity of cells and assess the metastatic potential of cancerous lesions based on the principle of fluorescence resonance energy transfer (FRET). This QD−Au nanocrystal structure was made using the same QD nanocrystals and the EDC coupling protocol described here.[38]

Bioactivity Tests of Water-Soluble Quantum Dots and Quantum Dot−Anti-Her2 Bioconjugates in Live Cell Molecular Targeting. The human breast cancer cell line SK-BR-3 (American Type Culture Collection, Manassas, VA) that overexpresses Her2 (positive control) was cultured (37 °C, 5% CO_2) on glass chamber slides (Nalge Nunc International, Rochester, NY) in McCoy's 5A medium with 10% (v/v) fetal bovin serum (FBS; Invitrogen Corp., Carlsbad, CA) overnight. The human breast cancer cell line MCF-7 (American Type Culture Collection) that is Her2 negative (negative control) was cultured (37 °C, 5% CO_2) on glass chamber slides in Eagle's Minimum Essential medium with BSS and 2 mM L-glutamine supplemented with 0.01 mg/mL bovine insulin (Sigma-Aldrich) and 10% (v/v) FBS overnight. The cultured SK-BR-3 and MCF-7 cells were first gently rinsed with cool PBS and blocked with PBS containing 2% (wt/vol) bovine serum albumin (BSA) for 5 min to avoid unspecific binding.

The cells were then incubated with 50 nM water-soluble QDs or QD−anti-Her2 bioconjugates in full growth media containing 3% (wt/vol) BSA for 1 h at 20 °C and gently rinsed 3 times with PBS and visualized. All images were collected using a Zeiss LSM 510 META NLO mounted on an Axiovert 200M inverted microscope (Carl Zeiss MicroImaging, Inc., Thornwood, NY) and coupled to a Coherent Chameleon tunable titanium:sapphire laser (Coherent Laser Group, Santa Clara, CA) for two-photon imaging. QDs were excited with a 458-nm argon laser for live cell imaging. In addition, 720-nm two-photon excitation of synthesized QDs for fixed cell imaging was successfully performed (images not shown). All images were 512 × 512 pixels with 12-bit pixel depth. Lambda emission scanning from 521−671 nm was performed using the META detector to verify the luminescence from QDs.

In Vitro Cytotoxicity of Water-Soluble Quantum Dots. Water-soluble QDs were added to full growth medium of confluent SK-BR-3 cells at various concentrations. Cells were incubated in the dark over 48 h with the water-soluble QDs. The cells were then gently washed with PBS and stained using a commercial LIVE/DEAD stain assay (Invitrogen) at different exposure times (up to 48 h). The cells were counted manually according to standard protocol to attain statistical significance. All images were collected using the Zeiss Axiovert 135 with a Nikon Coolpix 5000 digital camera and analyzed by ImagePro (Silver Spring, MD).

Results

Synthesis of Semiconductor and Iron Oxide Nanocrystals. For the semiconductor nanocrystals or quantum dots used here, we adapted a method reported by Peng et al.[40,49,50] This technique, referred to as successive ion layer adsorption and reaction (SILAR), forms high-quality core/shell structures of metal chalcogenides in ODE. We found that if we lower the shell growth temperatures, the reaction proceeds more slowly and hence provides more control over the shell thickness. For this work, 180 and 200 °C were chosen for the shell growth of

(45) Yavuz, C. T.; Mayo, J. T.; Yu, W. W.; Prakash, A.; Falkner, J. C.; Yean, S.; Cong, L.; Shipley, H. J.; Kan, A.; Tomson, M. B.; Natelson, D.; Colvin, V. L. *Science* **2006**, *314*, 964−967.
(46) Butter, K.; Bomans, P. H. H.; Frederik, P. M.; Vroege, G. J.; Philipse, A. P. *Nat. Mater.* **2003**, *2*, 88−91.
(47) Al-Somali, A. M.; Krueger, K. M.; Falkner, J. C.; Colvin, V. L. *Anal. Chem.* **2004**, *76*, 5903−5910.
(48) Krueger, K. M.; Al-Somali, A. M.; Falkner, J. C.; Colvin, V. L. *Anal. Chem.* **2005**, *77*, 3511−3515.
(49) Battaglia, D.; Blackman, B.; Peng, X. *J. Am. Chem. Soc.* **2005**, *127*, 10889−10897.
(50) Battaglia, D.; Li, J. J.; Wang, Y.; Peng, X. *Angew. Chem., Int. Ed.* **2003**, *42*, 5035−5039.

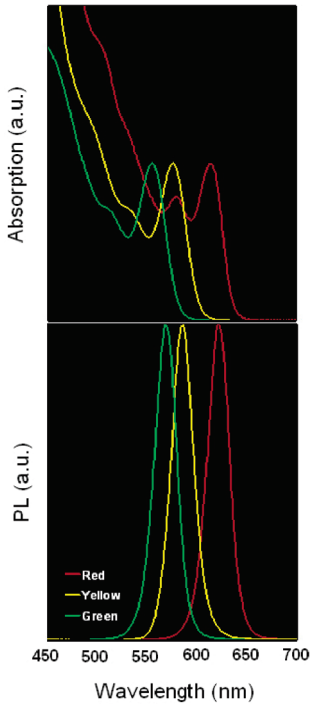

Figure 1. Top: UV−vis absorption spectra of three quantum dots with first excitonic absorption peaks of 613, 576, and 555 nm. The half width at half-maximum (to the right side) of the absorption peaks was 14 to 15 nm. Bottom: photoluminescence spectra of the three quantum dots (excited at 400 nm). The three quantum dots emitted red (peak position 621 nm), yellow (586 nm), and green (568 nm) lights with narrow peak width (full width at half-maximum) of 25 to 26 nm. The quantum yields for the three quantum dots were 55.5 (red), 50.6 (yellow), and 35.1% (green) (Rhodamine 640 was used as standard, and 100% quantum yield was adopted for it).

CdS or ZnS on a CdSe core resulting in three core/shell QDs with different colors (red, yellow, and green).

Absorption spectra showed the characteristic and narrow excitonic absorption peaks at 613, 576, and 555 nm for the red, yellow, and green QDs, respectively (Figure 1, top). Narrow PL spectra (25−26 nm for full width at half-maximum of the spectrum, fwhm) were recorded for these three QDs (Figure 1, bottom). The PL peak positions were 621, 586, and 568 nm for red, yellow, and green QDs, respectively. The quantum yields for emission were found by direct comparison with Rhodamine 640 (100% quantum yield) as 55.5, 50.6, and 35.1% for the red, yellow, and green materials. Transmission electron microscopy of dried samples revealed that these QDs were either nail-shaped (red QD, with CdS shell), or nearly spherical (yellow and green QDs, with ZnS shell) (Figure 2). For the red QDs, the dimensions were measured from TEM pictures through ImagePro as 5.8 nm (9.7% distribution) for the head width and 8.4 nm (14%) for the long axis. Several monodisperse iron oxide nanocrystals with different sizes were synthesized through the high-temperature decomposition of iron carboxylate salts in ODE.[44]

Formation of Amphiphilic Encapsulation Polymers and Quantum Dot Water Solubilization. The formation of PMAO−PEG was verified by FTIR characterization (Figure 3, left). The decrease of peak 1775 cm^{-1} and the increase of peak 1715 cm^{-1} were due to the decomposition of anhydride and the formation of −COOH. All the other characteristic vibrations from PMAO−PEG corresponded to those seen for mPEG−NH_2, the starting polymer. Figure 3 (right) shows that water-soluble nanocrystals exhibit the major characteristic IR peaks of the original QD (mainly oleate from oleic acid) and several new peaks that are similar to the free PMAO−PEG polymers.[51,52]

Once prepared, the PMAO−PEG copolymer can be used like a phase transfer agent; addition of the polymers to an oil and water mix of nanocrystals results in the complete transfer of the colored nanocrystals into the aqueous layer with the help of rotary evaporation. The solubilization process is rapid and occurs with 100% efficiency. After encapsulating the hydrophobic nanocrystals, the amphiphilic polymers have not only PEG chains available for biocompatibility but also free carboxylic acid groups available for further reaction. Carboxylic acid moieties are ideal for attaching biomolecules, such as peptides, proteins, antibodies, and nucleic acids, to the nanocrystal complexes through standard bioconjugation techniques.[53] PMAO and mPEG−OH polymers are commercially available at low price (∼$60/kg and $120−150/kg, respectively, and opposed to mPEG−NH_2, which is ∼$72 000/kg or higher), which suggests this method is suitable for large-scale production. It should be noted that PMAO itself, without further PEG derivatization, could also transfer QDs from chloroform into water if the pH was adjusted to 8−9 by sodium hydroxide initially (higher pH at this stage resulted in the decrease of quantum yield; a systematic study on this issue is in progress). Figure 4 (inset) shows two bottles of red QDs, one in chloroform (right) and one in pure water (left); the method also works for different QD sizes (red, yellow, and green) as shown in Figure S1.

Because this method leaves the surface coating of the QDs undisturbed, the optical properties before and after water solubilization are identical. Figure 4 shows no difference in the absorption and PL spectra of the materials in organic solvents and in water. Additionally, a quantitative measure of the quantum yields, with no photoactivation, of the water-soluble red (54.7%), yellow (50.6%), and green (34.5%) QDs was identical to those found before water solubilization.

Cryogenic techniques can be used to prepare frozen water solutions of quantum dots in which the solution-state dispersion and aggregation level are captured from the room temperature.[45,46] Transmission electron microscopy of these thin ice films thus can provide a means to evaluate nanocrystal aggregation directly in the liquid phase. Representative image from cryo-TEM is shown in Figure 5; nanocrystals appear well isolated and are rarely observed as aggregates.

The water-soluble QDs were very stable in water and physiological buffers. There was no precipitation in water over a wide pH range of 4−10 (adjusted by HCl or NaOH) and no optical density change in 10× PBS and 1 M NaCl solutions (pH 6−8) for nearly 2 years (currently available data). Samples were also stable in 1 M NaOH (pH 14) and 0.01 M HCl (pH 2) solutions for several hours depending on the molar ratio of PEG to PMAO and the chain length (molecular weight) of PEG used.[54] Further tests indicated that the water-soluble QDs were also stable at 70 °C while being sonicated over 3 h. The overall

(51) Kang, Y.; Seo, Y.-H.; Lee, C. *Bull. Korean Chem. Soc.* **2000**, *21*, 241−244.
(52) Atici, O. G.; Akar, A.; Rahimian, R. *Turk. J. Chem.* **2001**, *25*, 259−266.
(53) Hermanson, G. T. *Bioconjugate Techniques*; Academic Press: San Diego, CA, 1996.
(54) Li, Z.; Wei, L.; Gao, M. Y.; Lei, H. *Adv. Mater.* **2005**, *17*, 1001−1005.

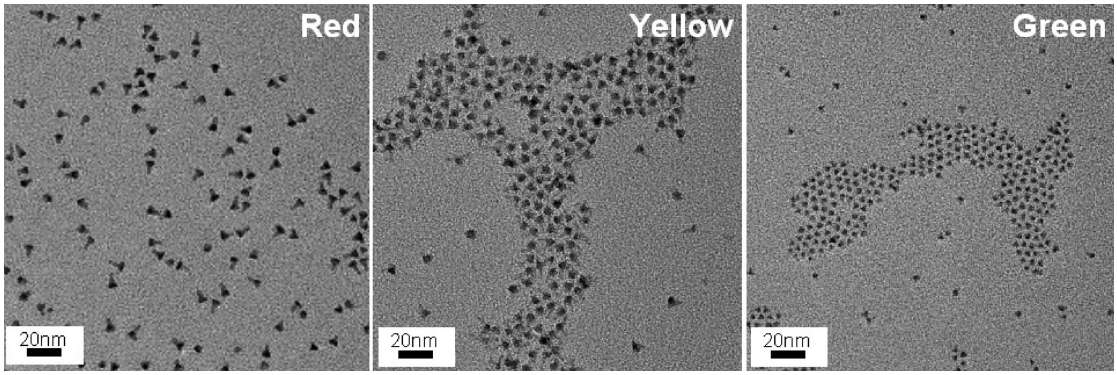

Figure 2. TEM photographs show that the size increased from green, yellow, to red quantum dots; the shapes also varied for different quantum dots due to the shell growth.

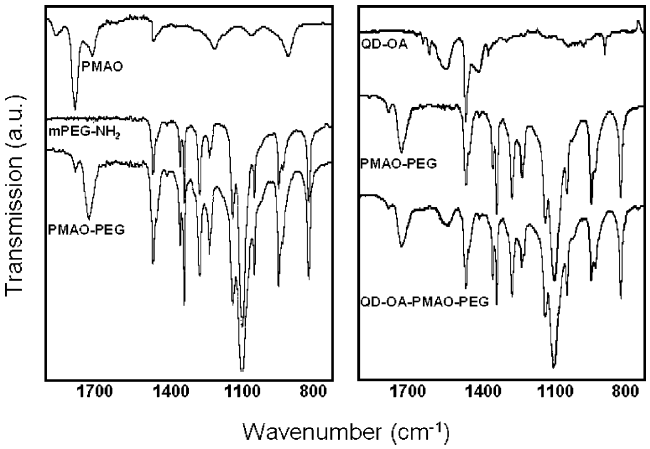

Figure 3. FTIR characterizations of PMAO−PEG (left) and water-soluble quantum dots (right).

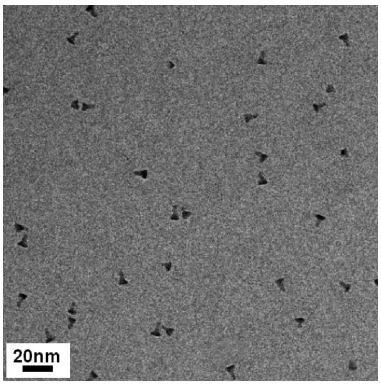

Figure 5. Cryogenic TEM photograph clearly shows the well-dispersed red water-soluble quantum dots in water. The size and shape were the same as the one in chloroform (Figure 2, red).

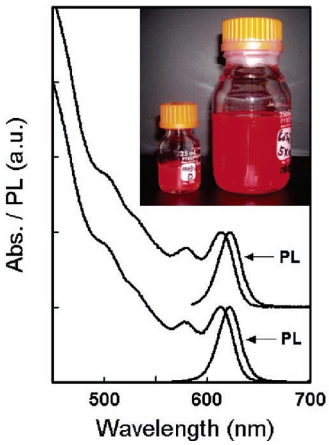

Figure 4. Comparisons of the absorption and photoluminescence spectra of red quantum dots in chloroform (top) and water (bottom). Both quantum dots had the same absorption and photoluminescence spectra. Inset: a visual comparison of red quantum dots in chloroform (right) and water (left) under room light.

stability is superior to reported results.[26,55,56] We have applied the same strategy to transfer other organic solvent-synthesized nanocrystals into water. For example, monodisperse PbSe semiconductor nanocrystals[15] and magnetic iron oxide nanocrystals[44] synthesized in ODE were successfully transferred into water. Figure S2 shows 9.6-nm iron oxide nanocrystals in chloroform (right) and water (left). These water-soluble iron oxide nanocrystals were extremely stable under a wide range of conditions including 2 M NaCl, 1 M NaOH, and 1 M HCl. We attribute the good stability of these water-soluble nanocrystals to the alternating structure of PMAO copolymers. The flexible backbone contains the PEG and octadecane components in a brushlike arrangement, which permits for ordered multiple interactions between the hydrophobic elements and the nanocrystals original coating (oleic acid, TOP, TOPO, etc.). Similar di- or triblock systems are not configured in this way and may limit the interactions between the hydrophobic tails and the nanocrystal surfaces. [1,31,56]

Bioactivity Tests of Water-Soluble Quantum Dots and the Quantum Dot−Bioconjugates in Living Cells. The as-prepared water-soluble QDs were exposed to a human breast cancer cell line SK-BR-3 which has the Her2 receptor for 4 h; confocal microscopy showed that QDs were endocytosed by the cells (Figure 6, left). We then examined incubating the same cell line with QD−anti-Her2 bioconjugates (positive control) for 1 h and found that the bioconjugates efficiently labeled the cell membranes (targeted to Her2 receptors) (Figure 6, right). A short movie clearly demonstrates red QDs targeted to the surface of a SK-BR-3 human cell (Supporting Information). A SK-BR-3 control demonstrated no luminescence signal in the

(55) Jiang, W.; Mardyani, S.; Fischer, H.; Chan, W. C. W. *Chem. Mater*. **2006**, *18*, 872−878.
(56) Luccardini, C.; Tribet, C.; Vial, F.; Marchi-Artzner, V.; Dahan, M. *Langmuir* **2006**, *22*, 2304−2310.

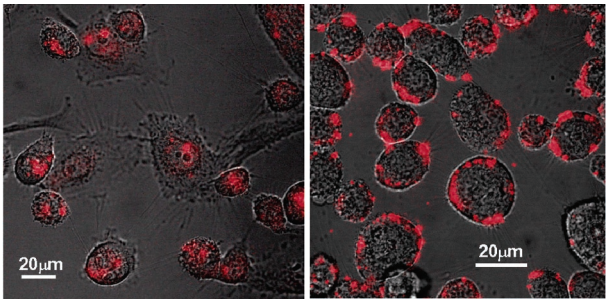

Figure 6. Left: live cell capture of red water-soluble quantum dots by SK-BR-3 human breast cells. Quantum dots were excited at 458 nm and visualized by confocal microscopy. Right: live cell targeting of Her2 receptor using quantum dot−anti-Her2 bioconjugates onto SK-BR-3 human breast cell membranes. Quantum dots were excited at 458 nm and visualized by confocal microscopy.

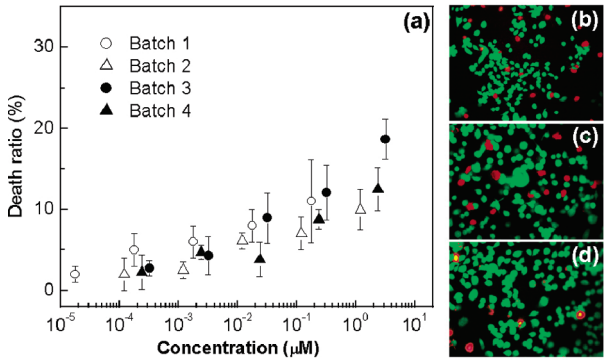

Figure 7. In vitro cytotoxicity of four different batches of red water-soluble quantum dots to SK-BR-3 human breast cells (a). There was little batch difference in cytotoxicity of the water-soluble quantum dots made by this strategy, and the cell death was below 10% with the quantum dot concentration up to 100 nM. The molar ratio of PMAO/PEG was 1:30, and the molecular weight of PEG was 6000. In vitro cytotoxicity of red water-soluble quantum dots with different polymer coatings [(b) pure PMAO, (c) PMAO−PEG with PEG MW of 750, (d) PMAO−PEG with PEG MW of 6000; molar ratio of PMAO/PEG was 1:10] to SK-BR-3 human breast cells (red spots are dead cells, green spots are live cells through a commercial LIVE/DEAD stain assay; 50 nM quantum dots were dosed to the cells). Death ratios for (b), (c), and (d) are 18.6, 11.4, and 10.9%, respectively ($p = 0.05$). The survival rate for control cells without exposed to quantum dots is 97% ± 3%.

range of 521−671 nm (Figure S3; red QDs emit at 621 nm). A negative control was performed by exposing QD−anti-Her2 bioconjugates to a human breast cancer cell line MCF-7 which has no Her2 receptors. This experiment found no emission stronger than the background in the same range of 521−671 nm, which confirmed that the successful targeting of the water-soluble QD−anti-Her2 bioconjugates (Figure S4) was indeed from the antibody−antigen interaction. We speculate that the use of PEG in the coating limited nonspecific binding and permitted cell receptors to access the anti-Her2 on the particle surface with high efficiency.[27]

Cytotoxicity of Water-Soluble Nanocrystals. Generally, research that has used QDs or iron oxide particles in applications such as biological imaging and detection has reported no significant effects on organisms over the duration of the experiments.[6,8,9,57] This observation is somewhat expected for the iron oxide materials, which have no molecular components that are toxic. On the other hand, the cadmium present in QDs could be extremely toxic to cells if the coatings permitted it to become bioavailable in a molecular form.[58,59] In some cases, the surface coatings are thought to prevent this from happening. For example, tumor cells labeled with QDs survived the circulation and extravasated into tissues just as effectively as unlabeled cells, and no difference in their ability to form tumors in mice was observed after 40 days.[60]

More focused studies of QD cytotoxicity, however, have determined that these materials at the appropriate dose will have adverse effects on cells.[35−37] The magnitude of the toxicity is critically dependent on the coating material. The release of free cadmium has been the subject of some debate, and either poor nanocrystal purification or incomplete surface capping may be the cause. For example, QDs coated with simple molecular capping groups, such as mercaptoacetic acid, mercaptopropionic acid, 11-mercaptoundecanoic acid, or 2-aminoethanethiol, were more toxic to cells than those coated with silica.[36,37] Toxicity could be reduced even further by the addition of PEG functionality to the surface.[35−37]

Our in vitro cytotoxicity study on the water-soluble QDs confirmed that when PEG coatings are used the materials show negligible toxicity to human breast cancer cells (SK-BR-3). Cancer cells were used here both because they are of interest in biomedical imaging using quantum dots and also because they are hardier than normal cell lines and thus a tougher screen for toxicity than normal cells. However, even among different normal cell lines such as skin fibroblasts and hepatocytes, there are varying grades of cell hardiness and resistance to cytotoxic environments, and thus these results cannot be generalized to set specific exposure limits. They are useful, however, for establishing a differential measure of toxic response to varying surface coatings.

Figure 7a shows that, when incubated with 100 nM water-soluble red QDs, less than 10% of the cells died after a 24-hour exposure. There was little batch difference in the cytotoxicity of the water-soluble QDs made by this strategy. Further cytotoxicity studies revealed that PEG does influence cytotoxicity. If the water-soluble QDs were made with PMAO only, 18.6% of the SK-BR-3 cells died after 24 h (Figure 7b). If there was PEG with PMAO, there was a statistically significant decrease in the toxicity (to about 10%). This observation was unaffected by the molecular weight of the PEG (750 to 20 000) (Figure 7c,d). We note that a more comprehensive differential cytotoxicity study of PEGylation and PEG chain length (molecular weight) has been published elsewhere.[34,39]

Discussion

Structure of Water-Soluble Quantum Dots. A central feature of this work is the generation of amphiphilic copolymers that are versatile, economical, and easily prepared. For all examples, the starting polymer is a commercially available PMAO, which is composed of maleic anhydride and octadecene monomers, alternatively. The octadecane component is compatible with the hydrophobic coatings already present on the nanocrystals, while the cyclic anhydride functionality is a coupling point for the addition of more polar polymers such as PEG. The anhydride group permits for a versatile attachment

(57) Michalet, X.; Pinaud, F.; Lacoste, T. D.; Dahan, M.; Bruchez, M. P.; Alivisatos, A. P.; Weiss, S. *Single Mol.* **2001**, *2*, 261−276.
(58) Celik, A.; Comelekoglu, U.; Yalin, S. *Toxicol. Ind. Health* **2005**, *21*, 243−248.
(59) Boudene, C.; Damerval, M. *Toxicol Eur. Res.* **1982**, *4*, 143−150.
(60) Voura, E. B.; Jaiswal, J. K.; Mattoussi, H.; Simon, S. M. *Nature Med.* **2004**, *10*, 993−998.

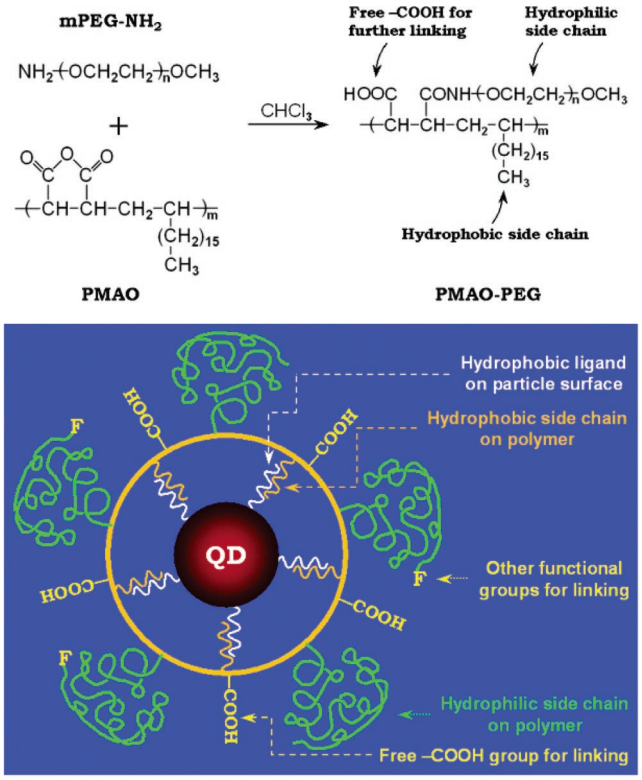

Figure 8. Top: one-step formation of PMAO−PEG amphiphilic polymers through reaction between maleic anhydride and amino groups. Bottom: schematic structure of water-soluble quantum dots (**F** stands for a functional group instead of $-OCH_3$, such as $-OH$, $-COOH$, $-NH_2$, etc.). Quantum dot particles were encapsulated by PMAO−PEG amphiphilic polymer hydrophobic interaction. Hydrophilic side chains of PEGs stayed exteriorly to make the whole structure soluble in water; carboxylic and **F** functional groups were used for bioconjugation.

chemistry that can link either PEG chains or amino−PEG to the base PMAO polymer. Figure 8 (top) illustrates the formation of PMAO−PEG polymers in chloroform through the reaction-between maleic anhydride and the free $-NH_2$ of a PEG$-NH_2$; a similar reaction for underivatized PEG is also possible though it requires more time and the addition of an acid catalyst.

Figure 8 (bottom) provides an illustration of the structure of the water-soluble QDs made by this approach. As stated above, the free $-$COOH groups in the polymer could be conjugated with biomolecules containing $-NH_2$ groups. The *F* functional group [such as $-$COOH and $-NH_2$ (comes from $-N_3$, tert-butyloxycarbonyl-, or 9-fluorenylmethoxycarbonyl-protected $-NH_2$[61,62]) instead of $-OCH_3$ in mPEG$-NH_2$ illustrated in Figure 8 (top)] is also available for bioconjugation. Figure 8 (bottom) furthermore reveals that different components other than PEG could be connected to PMAO either during the formation of PMAO-based amphiphilic polymers or after the formation of water-soluble QDs.

Incorporating PEG molecules to water-soluble nanocrystals can significantly increase the biocompatibility and reduce nonspecific binding.[27,33] It is reported that PEGylation of water-soluble QDs often resulted in the quantum yield decrease;[27] single PEG ligands (not linked to polymers) could induce spectra shifting.[63,64] Our one-step direct synthesis of amphiphilic polymers with PEGs not only eliminates the use of expensive coupling agents (e.g., EDC) and follow-up separations, but also avoids the quantum yield loss.

To evaluate the composition of the materials in more detail, we used thermogravimetric analysis (TGA) to determine the weight fraction of organic coatings in these materials. On the basis of simple geometric models (Figure 8, bottom), we expected that at full coverage the surface ligands (assuming oleate, from oleic acid, was the only ligand on the QD surface[12]) could be as much as 34% of the total weight in the core/shell structured red QD before polymer coating. TGA showed 36% loss, which was very close to our estimated ligand fraction. For the purified water-soluble QDs, the molar ratio of PMAO−PEG coating polymer to QD nanocrystal calculated from TGA is 1.04−1.25:1, assuming PMAO has an average MW of 40 000. This suggests that the PMAO backbones are not fully extended from the particle but rather wrap the QD surface so that the hydrophobic octadecane tails have maximum interactions with the oleate coatings on the nanocrystal surface. In another example, at least four triblock polymers (100 000 MW) were required to encapsulate a similar sized QD; this was probably due to the polymer's block structure where the noneffective blocks may form void loops. [31] It is clear that the polymer structure and flexibility will be important in determining the geometry of its interaction with a nanocrystal surface.

Hydrodynamic Diameter of Water-Soluble Quantum Dots. Although the quantum dot itself is the functional component, the amphiphilic polymer contributes a large fraction to the overall hydrodynamic diameter as well as chemical composition. Figure S5 shows the TEM images of a dried layer of PMAO−PEG nanocrystals obtained by negative staining of phosphotungstic acid. These images illustrate that there is only one QD particle inside a polymer shell and that apparently cross-linking between QDs does not occur. The diameter for the entire red water-soluble QD assembly, including the polymer layer, was 17 ± 5 nm measured from these images. This value is obviously smaller than the real hydrodynamic diameter in water because the polymer coatings shrink substantially upon drying.[65]

We then measured the hydrodynamic diameters of the red water-soluble QDs (molar ratio of PMAO/PEG was 1:10) with PEG MW of 750, 2000, 6000, 9900, and 19 300, respectively, employing SEC.[47,48,66,67] Figure S6 shows an SEC chromatogram for water-soluble red QDs. The hydrodynamic diameter was obtained by correlating the retention time (8.7 min) with a calibration curve established from known standards. DLS was also used to confirm the hydrodynamic diameters of these water-soluble QDs (Figure S7).[26,55,56,63,68] The results from DLS and SEC are summarized in Table 1.

It can be seen from Table 1 that the hydrodynamic diameter (HD) of water-soluble QDs increases with the PEG molecular

(61) Fields, G. B.; Tian, Z.; Barany, G. In *Synthetic Peptides: A User's Guide*; Grant, G. A., Ed.; W. H. Freeman: New York, 1992; pp 81−86.
(62) Bodanszky, M. *Principles of Peptide Synthesis*, 2nd ed.; Springer-Verlag: Berlin, 1993.
(63) Boulmedais, F.; Bauchat, P.; Brienne, M. J.; Arnal, I.; Artzner, F.; Gacoin, T.; Dahan, M.; Marchi-Artzner, V. *Langmuir* **2006**, *22*, 9797−9803.
(64) Pinaud, F.; King, D.; Moore, H.-P.; Weiss, S. *J. Am. Chem. Soc.* **2004**, *126*, 6115−6123.
(65) Rubinstein, M.; Colby, R. H. *Polymer Physics*, 1st ed.; Oxford University Press: New York, 2003.
(66) Fisher, C. H.; Weller, H.; Katsikas, L.; Henglein, A. *Langmuir* **1989**, *5*, 429−432.
(67) Ding, S.-Y.; Jones, M.; Tucker, M. P.; Nedeljkovic, J. M.; Wall, J.; Simon, M. N.; Rumbles, G.; Himmel, M. E. *Nano Lett.* **2003**, *3*, 1581−1585.
(68) Narayanan, S. S.; Pal, S. K. *J. Phys. Chem. B* **2006**, *110*, 24403−24409.

Table 1. Hydrodynamic Diameter (HD) of Water-Soluble Red QDs

PEG MW	maximum estimated HD (nm)[a]	estimated HD (nm)[b]	HD as found from DLS (nm)	HD as found from SEC (nm)
750	24.2	18.8	24.0	29.7
2000	44.6	22.4	28.5	32.1
6000	109.6	29.0	38.7	37.2
9900	173.0	33.2	42.1	39.5
19300	326.0	40.4	45.9	42.4

[a] The maximum size was taken as the core diameter, plus twice the thickness of the hydrophobic coating ($1.8 \times 2 = 3.6$ nm), plus twice the thickness of the PEG encapsulating polymer. For this maximum estimate, the PEG was assumed to be fully extended with a monomer-to-monomer distance. For 750 MW PEG, which contains 17 monomer units, this corresponded to a chain length of 6.1 nm. [b] This estimated size was found by taking the core diameter, plus twice the thickness of the hydrophobic coating, plus twice the thickness of the encapsulating polymer. In this case, however, the PEG was assumed to be a coiled chain and its hydrodynamic diameter was estimated from ref 69.

weight used; the two measurements (DLS and SEC) give very close HD values for all five water-soluble QD nanocrystals with different PEGs (columns 4 and 5). The measured HDs are distinct from those calculated from two different limits expected for the polymer structure (columns 2 and 3). In one case, we calculated the over HD assuming the PEG moieties adopt the same configuration as they do as a single, free component in water (called the "coil" model).[69] This model underestimates the size of the nanocrystal−polymer assembly because when bound to the surface the PEG polymers actually extend by 20−30% over their native structure. The extension of polymers when bound to both flat surfaces and larger nanoparticles is well established and arises from the steric crowding of polymers interfaces.[70−72] The other limiting structure is of a fully extended PEG chain (column 2). The measured hydrodynamic diameters, except for the shortest PEG, are smaller than the extended model, again in good agreement with studies of polymer brushes at interfaces. This difference becomes less pronounced for shorter molecular weight capping agents. Furthermore, the hydrodynamic sizes of QDs increase by 15−20 nm if they are conjugated with antibodies (anti-EGFR and anti-Her2), because antibodies (typically with a molecular weight near 150 000) have a hydrodynamic size of about 10 nm.[73,74]

Concentration Determination of Quantum Dot Solutions. The determination of quantum dot concentration in water is not straightforward; measurements of optical density can in principle be used to find molar concentrations if there are established absorption coefficients for these materials. However, the published extinction coefficients for quantum dots vary by more than an order of magnitude.[33,41−43] These discrepancies may arise in part from the sensitivity of absorption coefficients to both quantum dot diameter and composition. Additionally, even if these parameters are accounted for, any measurement of absorption coefficient must rely on secondary methods to determine the molar concentration in the test solutions. Dissolution of nanocrystals, followed by measurements of the atomic cadmium concentration, is one approach to such a measurement. However, converting such atomic measures into particle numbers requires models for nanoparticle structure and composition whose uncertainty introduces substantial errors.

For these samples, we applied the simple optical absorption method to evaluate the concentration of the quantum dot solutions. We measured the optical density of our core/shell structured QDs in water and then applied an absorption coefficient that was the average of three reported in the literature.[41−43] Using Lambert−Beer's law, $A = \epsilon bC$, where A is the optical density, b is the light path length, and C is the core/shell QD concentration, we then found concentration. Using this analysis, we found that the red QD solution shown in Figure 5 has a concentration of 19 ± 8.9 μM, assuming an extinction coefficient of $170\,000 \pm 80\,000$ μM cm^{-1}. The large error bar on the extinction coefficient means that optical absorption can at best give concentrations that are only accurate to 50%.

Alternatively, cryogenic TEM offers a direct and independent check on the approximate nanocrystal concentrations in aqueous phases. Cryogenic techniques are used to prepare thin ice films from water solutions by which the solute concentration and dispersion are not disturbed due to the quick freezing by liquid nitrogen.[45,46] In this way, we could collect images of solutions and provide a measure of the particle number density by counting the particles present in a known volume of ice. Assuming an ice thickness of 80 ± 20 nm (Vitrobot FP5350/60, FEI) and counting more than 2000 particles (total nanocrystal number from at least 40 images from different areas of the cryo-TEM grids; Figure 5), we arrive at a concentration of 12 ± 3.5 μM for the same red QD solution mentioned above. This method is especially useful when the nanocrystals have irregular shapes or lack characteristic parameters such as the extinction coefficients. While these two independent tests are in good agreement, current efforts are underway to develop more standard and accurate methods to determine this critically important parameter for biomedical applications.

Summary

A simple but effective and versatile method based on commercially available, low cost materials was developed to transfer the high-quality organic solvent-synthesized nanocrystals (UV−visible to NIR quantum dots and magnetic iron oxide nanocrystals tested) into water completely. The as-prepared water-soluble nanocrystals were very stable and preserved the same properties as the ones in organic solvents, such as the same absorption, the same photoluminescence, and the same quantum yield for QDs. Such amphiphilic polymer coatings have expanded the versatility of conjugation schemes, and we have recently reported methods to conjugate various biomolecules to make protease-activated quantum dot probes.[38] Very important parameters, such as hydrodynamic diameter and nanocrystal concentration, were measured for nanocrystal−polymer assemblies of varying sizes and compositions. These critical features are not easily characterized and are best obtained using several complementary tools.

Acknowledgment. This work was supported by the National Science Foundation through the Center for Biological and

(69) Mori, S.; Barth, H. G. *Size Exclusion Chromatography*, 1st ed.; Springer: Berlin, 1999.
(70) Field, J. B.; Toprakcioglu, C.; Ball, R. C.; Stanley, H. B.; Dai, L.; Barford, W.; Penfold, J.; Smith, G.; Hamilton, W. *Macromolecules* **1992**, *25*, 434−439.
(71) Karim, A.; Satija, S. K.; Douglas, J. F.; Ankner, J. F.; Fetters, L. J. *Phys. Rev. Lett.* **1994**, *73*, 3407−3410.
(72) Savin, D. A.; Pyun, J.; Patterson, G. D.; Kowalewski, T.; Matyjaszewski, K. *J. Polym. Sci., Part B: Polym. Phys.* **2002**, *40*, 2667−2676.
(73) Murphy, R. M.; Slayter, H.; Schurtenberger, P.; Chamberlin, R. A.; Colton, C. K.; Yarmush, M. L. *Biophys. J.* **1988**, *54*, 45−56.
(74) Chen, J.; Zhou, L. Effect of storage conditions on IgG. www.malvern.co.uk/common/downloads/campaign/MRK703-01.pdf, accessed Nov. 2006.

Environmental Nanotechnology (EEC-0118007), the Food and Drug Administration (222-05-2003 TPA), and the Office of Naval Research (N00014-04-1-003).

Supporting Information Available: A picture of water-soluble QDs emitting green, yellow, and red lights, a picture of monodisperse iron oxide nanocrystals dispersed in chloroform and water, images of staining TEM, a SEC chromatogram, and an HD histogram of red water-soluble QDs, demonstrations of specificity and binding of red water-soluble QD−anti-Her2 conjugates to SK-BR-3 and MCF-7 breast cancer cells, and a short video in AVI format showing red water-soluble QD targeted to an SK-BR-3 breast cancer cell. This material is available free of charge via the Internet at http://pubs.acs.org.

JA067184N